Elastomers and Composites
Vol. 56, No. 2, pp. 92~99 (June 2021)

Print ISSN 2092-9676/Online ISSN 2288-7725
DOI: https://doi.org/10.7473/EC.2021.56.2.92

Change of Crystalline Properties of Poly(ethylene-*co*-vinyl acetate) according to the Microstructures

Sung-Seen Choi† and Yu Yeon Chung

Department of Chemistry, Sejong University, 209 Neungdong-ro, Gwangjin-gu, Seoul 05006, Republic of Korea

(Received June 16, 2021, Revised June 28, 2021, Accepted June 30, 2021)

Abstract: Microstructure-dependent changes in the crystalline properties of poly(ethylene-*co*-vinyl acetate) (EVA) was investigated using various EVAs at different VA contents via X-ray diffraction (XRD). The parameters analyzed herein were percentage crystallinity ($\mathbf{X_c}$), interplanar crystal spacing (d_{hkl}), crystal stack size (D_{hkl}), and the number of crystal plane piles (N_{hkl}). The $\mathbf{X_c}$s of [110] and [200] crystals were 21.0-4.1 and 6.7-1.4%, respectively, and they decreased by approximately 2.3 and 0.7% for every mol% of the VA content, respectively. The $\mathbf{X_c}$ ratios of the [110] and [200] crystals were approximately 3. The d_{110}s and d_{200}s values were 0.41-0.42 and 0.37-0.38 nm, respectively. The D_{110}s and D_{200}s values were 9.56 -21.92 and 7.00-16.42 nm, respectively. The d_{hkl}s increased with an increase in the VA content, whereas the D_{hkl}s decreased. The N_{110}s and N_{200}s were 22.7-51.3 and 18.3-43.2, respectively, and they decreased by increasing the VA content. EVA with the same VA content showed different crystalline properties as per the suppliers, and some EVAs deviated from the average trends. This could be explained by the difference in their microstructures such as the sizes and distribution uniformity of the ethylene sequences in EVA chains.

Keywords: poly(ethylene-*co*-vinyl acetate), crystalline properties, microstructures, X-ray diffraction

Introduction

Poly(ethylene-*co*-vinyl acetate) (EVA) is a copolymer of ethylene and vinyl acetate (VA), and the VA units are randomly distributed throughout the ethylene polymer backbone. EVA is a transparent thermoplastic copolymer, and it becomes more flexible and transparent by increasing the VA content. EVA has crystalline structures due to the ethylene sequences, and its properties and application fields are mainly depending on the VA content.[1-6] The crystalline structures are influenced by the VA units (Scheme 1). Crystallinity and melting points of EVA decrease with increase in the VA content.[7] X-ray diffraction (XRD) and differential scanning calorimetry (DSC) are common analysis techniques to investigate crystalline properties of polymeric materials.[8-22] It is well known that degree of crystallinity influences on properties of polymers, and XRD is widely used for analysis of the crystallinity of polymeric materials.

Length of the ethylene sequence of EVA is restricted by positions of the VA units as shown in Scheme 2. Paraffin wax has stacked lamella crystals due to relatively short methylene sequence, while polyethylene (PE) has chain-folding crystalline structures due to long methylene sequence.[23-27] EVA should have stacked lamella crystals like paraffin wax because of relatively small ethylene block size. In general, EVAs have two crystalline structures of [110] and [200]. Crystalline structure and ethylene block size of an EVA should be influenced not only by the VA content but also by positions of the VA units in an EVA chain. Thus, crystalline structures and ethylene block sizes of EVAs with the same VA content may be different each other if the distribution patterns (or uniformities) of the VA units are different as described in Scheme 2.

In this study, crystalline properties of various EVAs with the VA contents of 3.3-17.8 mol% (9.5-40 wt%) were analyzed using XRD and influence of microstructures of the EVAs on the crystalline properties was investigated. Percentage crystallinity ($\mathbf{X_c}$), interplanar crystal spacing (d_{hkl}), and crystal stack size (D_{hkl}) were compared as the crystalline properties. Three sets of EVAs having the same VA contents were employed to examine the influence of microstructures on the crystalline properties in detail. Relative superiority for the percentage crystallinity and the number of crystal plane

†Corresponding author E-mail: sschoi@sejong.ac.kr

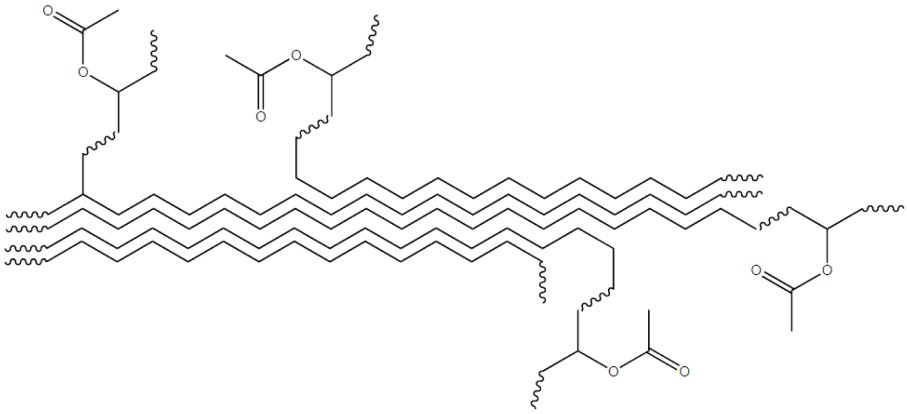

Scheme 1. Crystalline structure formed by the ethylene block of EVA.

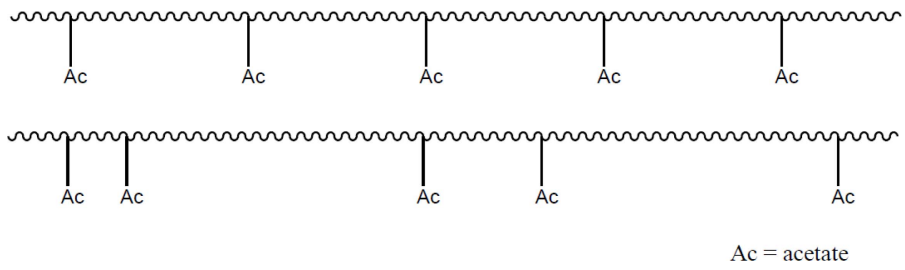

Scheme 2. Microstructures of EVA depending on the positions of vinyl acetate units.

piles (N_{hkl}) of [110] and [200] crystals was also investigated.

Experimental

Twelve EVAs with different VA contents of three suppliers were used: four EVAs of Aldrich Co. (USA) (marked to EVA 12, EVA 18, EVA 25, and EVA 40 with the VA contents of 12, 18, 25, and 40 wt%, respectively), four EVAs of DuPont Co. (USA) (EVA 770, EVA 450, EVA 360, and EVA 265 with the VA contents of 9.5, 18, 25, and 28 wt%, respectively), and four EVAs of Hanwha Co. (Republic of Korea) (EVA 1315, EVA 1316, EVA 1317, and EVA 1328 with the VA contents of 15, 18, 22, and 28 wt%, respectively). Weight percentages (wt%) of the VA contents were converted to the mole percentages (mol%) (Table 1). Three EVAs of EVA 18, EVA 450, and EVA 1316 have the same VA content of 6.7 mol%. Two sets of EVAs (EVA 25/EVA 360 and EVA 265/EVA 13128) have the same VA contents of 9.8 and 11.2 mol%, respectively.

Crystalline properties of EVA samples were measured using XRD. XRD analysis was performed using a D-max 2500/PC diffractometer (Rigaku Co., Japan) with Cu-K_α radiation. The accelerating voltage and electric current were 40 kV and 100 mA, respectively. The samples were scanned from 10° to 35° at a scan speed of 2°/min. The degree of crystallinity determined by XRD was calculated as the percentage of the scattered intensity of the crystalline phase over the sum of the scattered intensities of the crystalline and amorphous phases. The percentage crystallinity was acquired from the peak at 12° to 28° using XRD analysis software (Mdi Jade 6.0).

The percentage crystallinity ($\mathbf{X_c}$, %) was calculated using equation (1).

Table 1. EVAs Used in This Study

EVA	Vinyl acetate content (mol%)
EVA 770	3.3
EVA 12	4.3
EVA 1315	5.4
EVA 18	6.7
EVA 450	6.7
EVA 1316	6.7
EVA 1317	8.4
EVA 25	9.8
EVA 360	9.8
EVA 265	11.2
EVA 1328	11.2
EVA 40	17.8

$$\mathbf{X_c}\ (\%) = 100 \times \mathbf{I_c}/(\mathbf{I_c} + \mathbf{I_a}) \quad (1)$$

where $\mathbf{I_c}$ and $\mathbf{I_a}$ are the sums of the intensities of the crystalline and amorphous regions, respectively. The interplanar crystal spacing of (*hkl*) planes, d_{hkl} was calculated according to Bragg's law of equation (2).

$$d_{hkl} = \lambda/2\sin\theta \quad (2)$$

where λ is the wavelength of the X-ray (Cu-K_α = 0.154 nm) and θ is the Bragg angle. The stack (or particle) size of crystal was calculated according to Scherrer formula of equation (3).

$$D_{hkl} = K\lambda/(B_{1/2}\cos\theta) \quad (3)$$

where D_{hkl} is the interfacial distance (perpendicular to the plane of the crystal particle), K is the Scherrer constant (0.89 is selected), λ is the wavelength of the X-ray, $B_{1/2}$ is the FWHM (radian), and θ is the Bragg angle.

Results and Discussion

Raw XRD pattern was smoothed for following deconvolution process to separate the crystalline and amorphous regions. The smoothed curve was deconvoluted to one amorphous and two crystalline peaks as shown in Figure 1. Two crystalline peaks at 2θ = 21.4 and 23.7° corresponding to [110] and [200] crystals, respectively, were observed. Full width at half maximum (FWHM) of the crystalline peak was also measured. The Bragg angles (2θ) and FWHMs of EVAs were summarized in Table 2. Ranges of the Bragg angles of

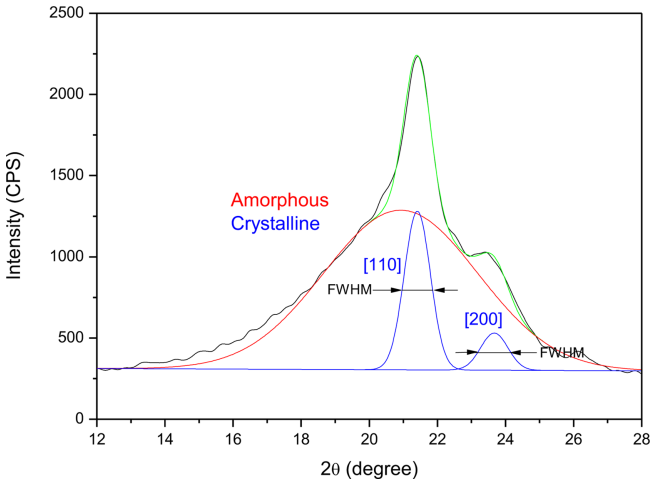

Figure 1. XRD pattern and deconvolted peaks of EVA 18. The XRD pattern was deconvoluted into the amorphous and crystalline peaks. FWHM denotes the full width at half maximum of the peak.

Table 2. Bragg Angles (2θ) and FWHMs of EVAs Obtained from the XRD Analysis Results (°)

EVA	2θ		FWHM	
	[110]	[200]	[110]	[200]
EVA 12	21.45	23.68	0.765	1.191
EVA 18	21.42	23.40	0.919	0.978
EVA 25	21.62	23.92	1.028	1.112
EVA 40	21.04	23.26	1.672	2.294
EVA 770	21.68	23.88	0.761	1.032
EVA 450	21.44	23.56	0.924	1.049
EVA 360	21.66	23.78	0.924	1.249
EVA 265	21.24	23.48	0.936	1.195
EVA 1315	21.44	23.54	0.844	1.220
EVA 1316	21.54	23.86	0.878	1.195
EVA 1317	21.26	23.61	1.141	1.195
EVA 1328	21.10	23.31	1.178	1.605

[110] and [200] peaks were 21.04-21.68 and 23.26-23.92°, respectively. Ranges of the FWHMs of [110] and [200] peaks were 0.76-1.67 and 0.99-2.29°, respectively. The FWHMs of [110] peaks were narrower than those of [200] ones. The FWHM of [110] peak tended to increase as the VA content increased.

The $\mathbf{X_c}$ variation with the VA content was plotted as shown in Figure 2. The total $\mathbf{X_c}$ of [110] and [200] crystals decreased by about 3% every 1 mol% of the VA content. The individual $\mathbf{X_c}$s of [110] and [200] crystals decreased by about

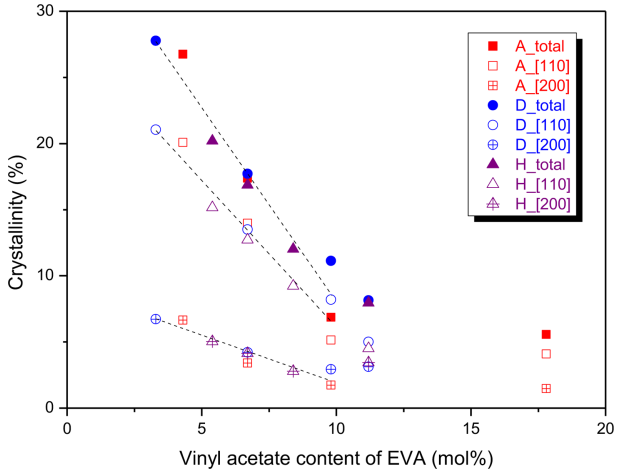

Figure 2. Variation of the total, [110], and [200] crystallinities of EVA with the vinyl acetate content. The squares, circles, and triangles stand for the EVAs of Aldrich Co., DuPont Co., and Hanwha Co., respectively. The solid, open, and crossed symbols indicate the total, [110], and [200] crystallinities, respectively. The three dash lines are the curve fitted lines less than 10 mol% of the vinyl acetate content for the total, [110], and [200] of y = -2.98x + 37.68 (r = 0.975), y = -2.27x + 28.61 (r = 0.977) and y = -0.72x + 9.06 (r = 0.945), respectively.

2.3 and 0.7%/mol%, respectively. After 10 mol% of the VA content, the decrement was very slight. There were some cases largely deviated from the fitted curve. For EVAs with 9.8 mol% of the VA content (EVA 25 and EVA 360), the $\mathbf{X_c}$s of EVA 25 were lower than the fitted line but those of EVA 360 were much higher than the fitted line. If the VA units are evenly distributed, there will be few large ethylene blocks and crystalline structures may not be well developed. If the VA units of an EVA with 10.0 mol% of the VA content are absolutely evenly distributed, the ethylene block size is '9' of ~VA-$(CH_2CH_2)_9$-VA~. Difference in the melting points of paraffin wax and its ester is about 15°C, and the total number of ethylene units not to participate in crystal formation by the prevention of VA units in both sides is about '8'.[28,29] Thus, the number of ethylene sequence to participate in the crystal formation is just '1' for an EVA with the VA content of 10.0 mol% when the VA units are completely evenly distributed. Hence, it can be expected that distribution uniformity of the VA units of EVA 25 will be greater than that of EVA 360.

There are two crystalline structures of ethylene blocks of ~VA-$(CH_2CH_2)_n$-VA~ (n > 20 and 15 < n < 20) in EVA.[29] The large and small ethylene block sizes may belong to the [110] and [200] crystals, respectively. The $\mathbf{X_c}$ ratio of [110] and [200] crystals ($\mathbf{X_c}$[110]/$\mathbf{X_c}$[200]) was plotted as a function of the VA content as shown in Figure 3. The $\mathbf{X_c}$ ratio on the whole slightly decreased with increase in the VA content. It means that crystal formation of the big ethylene block was more decreased than that of the small one by increasing the VA content. Except for three EVAs (EVA 18, EVA 265, and EVA 1328), the $\mathbf{X_c}$ ratios were about 3. The $\mathbf{X_c}$ ratio of EVA 18 (6.7 mol% of the VA content) was larger than those of the other EVAs. This is because EVA 18 has higher [110] crystallinity as well as lower [200] one compared to the other EVAs with the same VA content as shown in Figure 2. This implies that there are longer ethylene sequences in EVA 18 due to more inhomogeneous distribution of the VA units. The $\mathbf{X_c}$ ratios of EVA 265 and EVA 1328 (their VA contents are the same of 11.2 mol%) were much lower than those of the other EVAs since they had relatively higher $\mathbf{X_c}$s of the [200] crystal. Thus, EVA 265 and EVA 1328 should have more homogeneous distribution of VA units than the other EVAs.

Variations of the d_{hkl} and D_{hkl} were plotted as a function of the VA content as shown in Figures 4 and 5, respectively. The d_{110}s and d_{200}s were 0.410-0.422 and 0.372-0.382 nm, respectively (Figure 4). The d_{110}s were greater than the d_{200}s and the difference was about 0.04 nm. The d_{110} and d_{200} on the whole increased as the VA content increased, and the increment of d_{110} was slightly larger than that of d_{200}. This means that distance between EVA chains becomes longer by prevention of the VA units. The D_{110}s and D_{200}s were 9.564-21.918 and 6.997-16.417 nm, respectively (Figure 5). The D_{110} was greater than the D_{200}, and the difference became smaller by increasing the VA content. The D_{110} and D_{200} on the whole decreased with increase in the VA content, and the decrement of D_{110} was greater than that of D_{200}. The decreased D_{hkl}s can be explained by reduction of the number of ethylene sequences participating in the crystal formation. Some EVAs of the same supplier had similar D_{hkl}s though

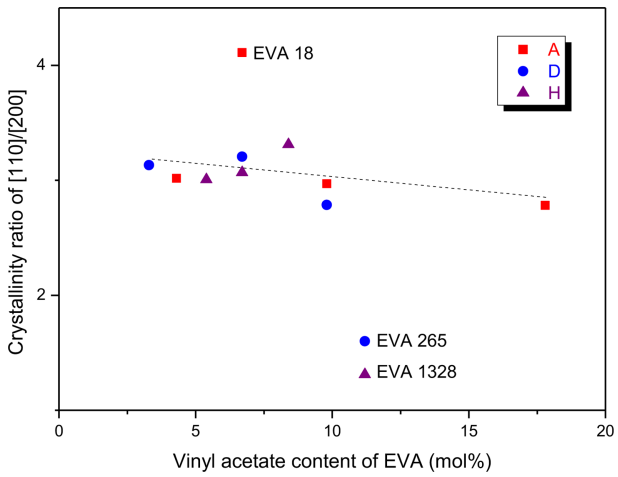

Figure 3. Variations of the crystallinity ratio of [110]/[200] of EVA with the vinyl acetate content.

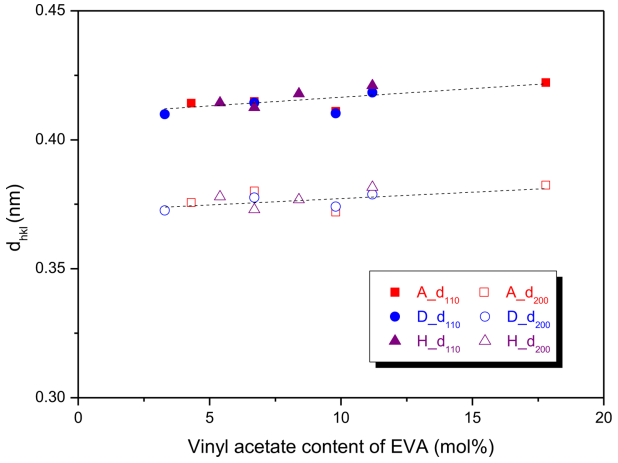

Figure 4. Variations of the interplanar crystal spacings (d_{hkl}s) with the vinyl acetate content. The squares, circles, and triangles stand for the EVAs of Aldrich Co., DuPont Co., and Hanwha Co., respectively. The solid and open symbols indicate the d_{110} and d_{200}, respectively. The dash lines are the curve fitted lines for the d_{110} and d_{200} of $y = 7.010 \times 10^{-4}x + 0.409$ (r = 0.637) and $y = 4.954 \times 10^{-4}x + 0.373$ (r = 0.485), respectively.

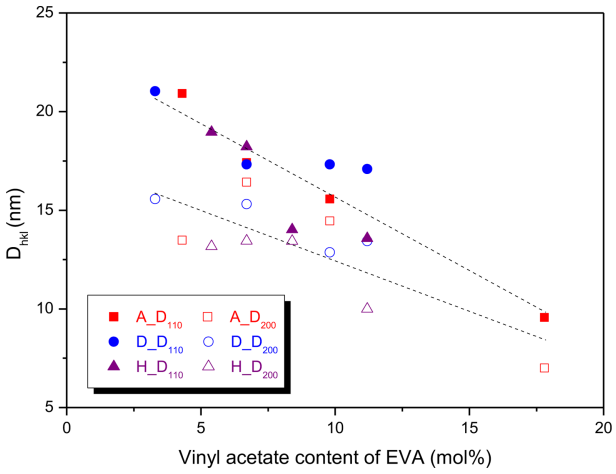

Figure 5. Variations of the interfacial distances (D_{hkl}s) with the vinyl acetate content. The squares, circles, and triangles stand for the EVAs of Aldrich Co., DuPont Co., and Hanwha Co., respectively. The solid and open symbols indicate the D_{110} and D_{200}, respectively. The dash lines are the curve fitted lines for the D_{110} and D_{200} of y = -0.751x + 23.092 (r = 0.901) and y = -0.522x + 17.625 (r = 0.782), respectively.

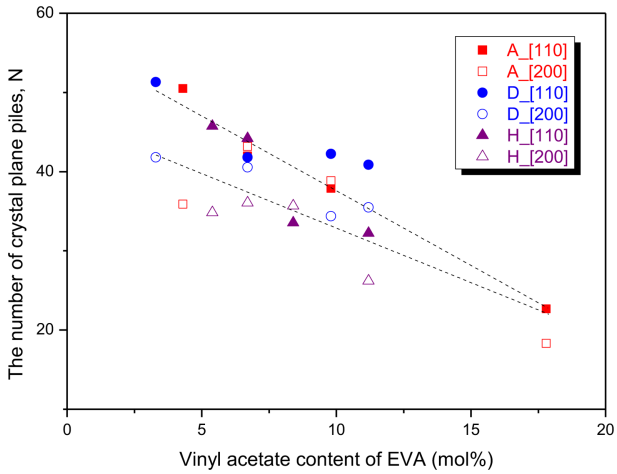

Figure 6. Variations of the numbers of crystal plane piles (N_{110} and N_{200}) of the [110] and [200] crystalline peaks of EVA with the vinyl acetate content. The squares, circles, and triangles stand for the EVAs of Aldrich Co., DuPont Co., and Hanwha Co., respectively. The solid and open symbols indicate the crystalline structures of [110] and [200], respectively. The dash lines are the curve fitted lines for [110] and [200] crystals of y = -1.86x + 56.15 (r = 0.900) and y = -1.42x + 47.07 (r = 0.787), respectively.

their VA contents are very different. For instance, EVA 450, EVA 360, and EVA 265 (6.7-11.2 mol% of the VA content) had similar D_{110} of 17.32-17.09, and EVA 1315, EVA 1316, and EVA 1317 (5.4-8.4 mol% of the VA content) had similar D_{200} of 13.16-13.45. The D_{hkl}s of EVAs with the same VA content showed big difference according to the suppliers. For EVA 18, EVA 450, and EVA 1316 with the same VA content of 6.7 mol%, the order of D_{110} was EVA 1316 > EVA 18 ~ EVA 450, whereas that of D_{200} was EVA 18 > EVA 450 > EVA 1316. For EVA 25 and EVA 360 with the VA content of 9.8 mol%, the D_{110} of EVA 360 was greater than that of EVA 25, whereas the D_{200} of EVA 360 was smaller than that of EVA 25. Thus, it can lead to a conclusion that the D_{hkl}s are largely influenced by the VA content and the distribution uniformity of VA units.

The number of crystal plane piles (N_{hkl}) was calculated using equation (4).[30]

$$N_{hkl} = D_{hkl}/d_{hkl} \quad (4)$$

The N_{110}s and N_{200}s were 22.7-51.3 and 18.3-43.2, respectively. Figure 6 shows variations of the N_{110} and N_{200} with the VA content. The N_{110} decreased with increase in the VA content by about twice every 1 mol% of the VA content, and it will be lower than 10 when the VA content is higher than 24.8 mol%. This implies that not only the ethylene block size but also the number of EVA chains participating in the [110] crystal formation decreased by increasing the VA content. The N_{200} did not show notable change until about 10 mol% of the VA content and then showed a decreased trend. The N_{110}s were generally larger than the N_{200}s, but EVA 18, EVA 25, and EVA 1317 showed the reverse trends. The larger N_{110}s than N_{200}s implies that the number of EVA chains with long ethylene sequences is greater than that of EVA chains with short ones. On the contrary to this, for EVA 18, EVA 25, and EVA 1317, the number of EVA chains with long ethylene sequences might be smaller than that of EVA chains with short ones.

The N_{110}s and N_{200}s of EVAs with the same VA content also showed different trends according to the suppliers. For EVA 18, EVA 450, and EVA 1316 with the same VA content of 6.7 mol%, the N_{110} of EVA 1316 was greater than those of the others whereas the N_{200} of EVA 1316 was smaller than those of the others. And total N_{hkl}s of the N_{110} and N_{200} were also different each other. The total N_{hkl}s of EVA 18, EVA 450, and EVA 1316 were 85.2, 82.3, and 80.3, respectively. Flexibility and transparency of EVA with smaller N_{hkl}s might be better than those of EVA with larger ones. For EVA 25 and EVA 360 with the same VA content of 9.8 mol%, the N_{110} of EVA 360 was greater than that of EVA 25 but the N_{200} of EVA 360 was smaller than that of EVA 25 though the total N_{hkl}s were the same of 76.7 and 76.6 for EVA 25 and EVA 360, respectively. For EVA 265 and EVA 1328 with the same VA content of 11.2 mol%, both the N_{110} and N_{200}

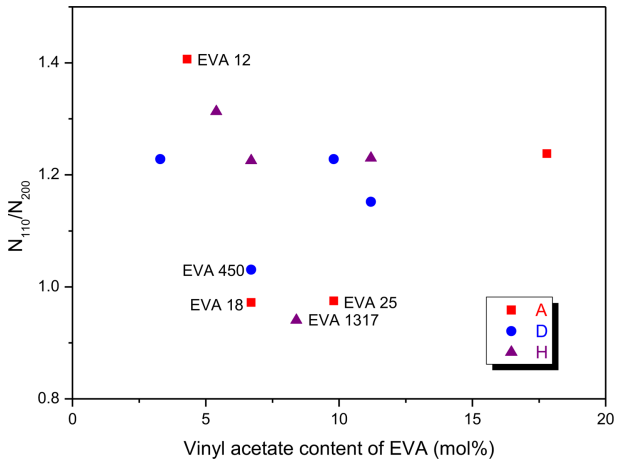

Figure 7. Variation of the N_{110}/N_{200} ratio with the vinyl acetate content. N_{110} and N_{200} are the numbers of crystal plane piles of [110] and [200], respectively. The squares, circles, and triangles stand for the EVAs of Aldrich Co., DuPont Co., and Hanwha Co., respectively.

of EVA 265 were greater than those of EVA 1328. The total N_{hkl} of EVA 265 (76.3) was greater than that of EVA 1328 (58.5) by 1.3 times. This denotes that EVA 1328 would be more flexible and transparent than EVA 265.

Figure 7 shows variation of the N_{110}/N_{200} ratio with the VA content. Except for some EVAs, the N_{110}/N_{200} ratios were about 1.2. This implies that the number of EVA chains participating in [110] crystal formation is greater than that of EVA chains participating in [200] one by about 20%. EVA 12 had the greatest N_{110}/N_{200} ratio of 1.41. The N_{110}/N_{200} ratios of EVA 450, EVA 18, and EVA 25 were nearly 1.00 (1.03, 0.97, and 0.98, respectively). The N_{110}/N_{200} ratio of EVA 1317 (0.94) was lower than the others. EVAs with the average low N_{110}/N_{200} ratio might have the long ethylene sequences less than the short ones. Especially, EVA 1317, EVA 25, and EVA 18 would have the long ethylene sequences less than the short ones as discussed previously.

Influence of the VA content and distribution uniformity of EVA on the crystalline properties was summarized in Table 3. The total $\mathbf{X_c}$ notably decreased by increasing the VA content, while it slightly decreased by increasing the distribution uniformity. The $\mathbf{X_c}$[110]/$\mathbf{X_c}$[200] ratio was more affected by the distribution uniformity than the VA content. The d_{110} and d_{200} slightly increased by increasing the VA content, but the distribution uniformity did not affect the d_{110} and d_{200}. The D_{110} and D_{200} decreased by increasing the VA content, whereas the D_{200} slightly increased by increasing the distribution uniformity. Variations of the N_{110} and N_{200} according to the VA content and distribution uniformity showed similar trends to those of the D_{110} and D_{200}. The N_{110}/N_{200} ratio slightly decreased by increasing the distribution uniformity, but the VA content did not affect the N_{110}/N_{200} ratio.

Table 3. Influence of the Microstructures on the Crystalline Properties of EVA*

Crystalline property	VA content	Distribution uniformity
Total crystallinity	↓↓↓	↓
$\mathbf{X_c}$[110]/$\mathbf{X_c}$[200]	↓	↓↓
d_{110}	↑	---
d_{200}	↑	---
D_{110}	↓↓	↓
D_{200}	↓	↑
N_{110}	↓	↓
N_{200}	↓	↑
N_{110}/N_{200}	---	↓

*↑: slightly increased, ---: not influenced, ↓: slightly decreased, ↓↓: decreased, ↓↓↓: largely decreased

Conclusions

Two crystalline peaks at 2θ = 21.0-21.7° and 23.2-24.0° of the [110] and [200] crystals of EVA were corresponded to the large and small ethylene block sizes, respectively. The $\mathbf{X_c}$ ratios of [110] and [200] were about 3 except for some EVAs, and it on the whole slightly decreased with increase in the VA content of EVA. The total $\mathbf{X_c}$ decreased by about 3%/mol%, while the individual $\mathbf{X_c}$s of [110] and [200] decreased by about 2.3 and 0.7%/mol%, respectively. Formation of the crystalline structures of EVA became more difficult by increasing the distribution uniformity. The d_{110}s and d_{200}s were 0.410-0.422 and 0.372-0.382 nm, respectively, and they on the whole increased as the VA content increased. The D_{110}s and D_{200}s were 9.564-21.918 and 6.997-16.417 nm, respectively, and they on the whole decreased with increase in the VA content. The N_{110}s and N_{200}s were 22.7-51.3 and 18.3-43.2, respectively, and the N_{110} decreased with increase in the VA content by about 2/mol%. The N_{110}/N_{200} ratios were about 1.2 except for some EVAs. For some EVAs, the crystalline properties were largely deviated from the average trends. EVAs with the same VA content of different suppliers showed some different crystalline properties. These were explained by difference in their microstructures, especially degree of the distribution uniformity. Difference in the crystalline properties due to the microstructures could influence on properties of EVAs such as flexibility and transparency.

References

1. S. Bistac, P. Kunemann, and J. Schultz, "Crystalline modifications of ethylene-vinyl acetate copolymers induced by a tensile drawing: effect of the molecular weight", *Polymer*, **39**, 4875 (1998).
2. S. Bistac and J. Schultz, "Influence of tensile deformation on the crystalline organization of ethylene copolymers", *J. Macromol. Sci. B Phys.*, **38**, 663 (1999).
3. X. M. Shi, J. Zhang, J. Jin, and S. J. Chen, "Non-isothermal crystallization and melting of ethylene-vinyl acetate copolymers with different vinyl acetate contents", *Exp. Polym. Lett.*, **2**, 623 (2008).
4. M. Alexandre, G. Beyer, C. Henrist, R. Cloots, A. Rulmont, R. Jerome, and P. Dubois, "Preparation and properties of layered silicate nanocomposites based on ethylene vinyl acetate copolymers", *Macromol. Rapid Commun.*, **22**, 643 (2001).
5. W. Zhang, D. Chen, Q. Zhao, and Y. Fang, "Effects of different kinds of clay and different vinyl acetate content on the morphology and properties of EVA/clay nanocomposites", *Polymer*, **44**, 7953 (2003).
6. V. Pasanovic-Zujo, R. K. Gupta, and S. N. Bhattacharya, "Effect of vinyl acetate content and silicate loading on EVA nanocomposites under shear and extensional flow", *Rheol. Acta*, **43**, 99 (2004).
7. C. Schneider, R. Langer, D. Loveday, and D. Haire, "Applications of ethylene vinyl acetate copolymers (EVA) in drug delivery systems", *J. Control. Rel.*, **262**, 284 (2017).
8. Y. Kong and J.N. Hay, "The enthalpy of fusion and degree of crystallinity of polymers as measured by DSC", *Eur. Polym. J.*, **39**, 1721 (2003).
9. P. Cebe, D. Thomas, J. Merfeld, B. P. Partlow, D. L. Kaplan, R. G. Alamo, A. Wurm, E. Zhuravlev, and C. Schick, "Heat of fusion of polymer crystals by fast scanning calorimetry", *Polymer*, **126**, 240 (2017).
10. J. E. K. Schawe, "Remarks regarding the determination of the initial crystallinity by temperature modulated DSC", *Thermochim. Acta*, **657**, 151 (2017).
11. N. S. Murthy and H. Minor, "General procedure for evaluating amorphous scattering and crystallinity from X-ray diffraction scans of semicrystalline polymers", *Polymer*, **31**, 996, (1990).
12. T. H. Lee, F. Y. C. Boey, and K. A. Khor, "X-ray diffraction analysis technique for determining the polymer crystallinity in a polyphenylene sulfide composite", *Polym. Compos.*, **16**, 481 (1995).
13. K. A. Moly, H. J. Radusch, R. Androsh, S. S. Bhagawan, and S. Thomas, "Nonisothermal crystallisation, melting behavior and wide angle X-ray scattering investigations on linear low density polyethylene (LLDPE)/ethylene vinyl acetate (EVA) blends: effects of compatibilisation and dynamic crosslinking", *Eur. Polym. J.*, **41**, 1410 (2005).
14. Y. Chen, H. Zou, M. Liang, and Y. Cao, "Melting and crystallization behavior of partially miscible high densitypolyethylene/ethylene vinyl acetate copolymer (HDPE/EVA) blends", *Thermochim. Acta*, **586**, 1 (2014).
15. X. Ju, M. Bowden, E. E. Brown, and X. Zhang, "An improved X-ray diffraction method for cellulose crystallinity measurement", *Carb. Polym.*, **123**, 476 (2015).
16. C. Motta, "The effect of copolymerization on transition temperature of polymeric materials, *J. Therm. Anal.*, **49**, 461 (1997).
17. W. Stark and M. Jaunich, "Investigation of ethylene/vinyl acetate copolymer (EVA) by thermal analysis DSC and DMA", *Polym. Test.*, **30**, 236 (2011).
18. X. M. Shi, J. Zhang, D. R. Li, and S. J. Chen, "Effect of damp-heat aging on the structures and properties of ethylene-vinyl acetate copolymers with different vinyl acetate contents", *J. Appl. Polym. Sci.*, **112**, 2358 (2009).
19. H. A. Khonakdar, S. H. Jafari, A. Haghighi-Asl, U. Wagenknecht, L. Haeussler, and U. Reuter, "Thermal and mechanical properties of uncrosslinked and chemically crosslinked polyethylene/ethylene vinyl acetate copolymer blends", *J. Appl. Polym. Sci.*, **103**, 3261 (2007).
20. K. Agroui, A. Maallemi, M. Boumaour, G. Collins, and M. Salama, "Thermal stability of slow and fast cure EVA encapsulant material for photovoltaic module manufacturing process", *Sol. Energy Mater. Sol. Cells*, **90**, 2509 (2006).
21. H. Varghese, T. Johnson, S. S. Bhagawan, S. Joseph, S. Thomas, and G. Groeninckx, "Dynamic mechanical behavior of acrylonitrile butadiene rubber/poly(ethylene-*co*-vinyl acetate) blends", *J. Polym. Sci. B: Polym. Phys.*, **40**, 1556 (2002).
22. A. Marcilla, J. A. Reyes-Labarta, and F. J. Sempere, "DSC kinetic study of the transitions involved in the thermal treatment of polymers. Methodological considerations", *Polymer*, **42**, 5343 (2001).
23. V. Chevallier, M. Bouroukba, D. Petitjean, M. Dirand, J. Pauly, J. L. Daridon, and V. Ruffier-Meray, "Crystallization of a multiparaffinic wax in normal tetradecane", *Fuel*, **79**, 1743 (2000).
24. H. S. Ashbaugh, A. Radulescu, R. K. Prudhomme, D. Schwahn, D. Richter, and L. J. Fetters, "Interaction of paraffin wax gels with random crystalline/amorphous hydrocarbon copolymers", *Macromolecules*, **35**, 7044 (2002).
25. I. A. M. Al-Raheil and A. M. Okaz, "Chain-folding in polyethylene lamellar structure", *Polym. Int.*, **28**, 261 (1992).
26. J. D. Hoffman and R. L. Miller, "Kinetic of crystallization from the melt and chain folding in polyethylene fractions

revisited: theory and experiment", *Polymer*, **38**, 3151 (1997).
27. D. L. Dorset and B. K. Annis, "Lamellar order and the crystallization of linear chain solid solutions", *Macromolecules*, **29**, 2969 (1996).
28. S. Patel, D. R. Nelson, and A. G. Gibbs, "Chemical and physical analyses of wax ester Properties", *J. Insect Sci.*, **1**, 4 (2001).
29. S-S Choi and Y. Y. Chung, "Simple analytical method for determination of microstructures of poly(ethylene-*co*-vinyl acetate) using the melting points", *Polym. Test.*, **90**, 106706 (2020).
30. J. Zhang, C. Wu, W. Li, Y. Wang, and Z. Han, "Study on performance mechanism of pour point depressants with differential scanning calorimeter and X-ray diffraction methods", *Fuel*, **82**, 1419 (2003).